JLISNT Journal of Leading Innovations in Science and Technology
Journal of Leading Innovations in Science and Technology, Vol.1, No.1, pp: 1-13, Jan 2026

Broadband mm-Wave Microstrip Antenna with Modified Patch and Ground Plane for 29-100 GHz High-Frequency Wireless Applications

Abhayinder Singh[1*], Ramyashree[2], U S Ajey[3]
[1,3]Manipal Institute of Technology, Manipal Academy of Higher Education, Manipal, India

*Correspondence: Abhayinder Singh, (abhayinder.mitmpl2022@learner.manipal.edu)

***Abstract*— A novel wideband millimeter-wave (mm-wave) microstrip antenna with modified radiating patch and defected ground structure is proposed for high-frequency wireless communication systems. The antenna is realized on Rogers RT-Duroid 5880 ($\varepsilon_r = 2.2$, $\tan\delta = 0.0009$) with compact dimensions of $80 \times 60 \times 1.5$ mm³. The measured results confirm an impedance bandwidth of 110%, covering the 29-100 GHz spectrum with $|S11| < -10$ dB. The antenna achieves a peak gain of 7.5 dBi and a peak radiation efficiency of 82%, maintaining stable far-field characteristics across the operating band. Excellent agreement between simulated and measured performance validates the design methodology. With its ultra-wideband response and reliable radiation performance, the antenna is well-suited for mm-wave 5G/6G communications, satellite links, automotive radar, imaging, and broadband sensing applications.**

***Index Terms*—** Wideband Antenna; mm-wave; 5G; 6G; Satellite Links; Broadband Sensing.

I. INTRODUCTION

The rapid growth of high-speed wireless networks has intensified the need for antennas capable of operating at millimeter-wave (mm-wave) frequencies. With 5G and emerging 6G systems relying on the 28-100 GHz spectrum, antennas must support wide bandwidth, low latency, and compact integration while maintaining strong radiation performance. These frequencies are essential for applications such as satellite communication, automotive radar, high-resolution imaging, and broadband sensing.

Conventional microstrip antennas struggle at such high frequencies due to limited bandwidth, efficiency, and design scalability. Recent research shows that modifying patch geometries and incorporating defected ground structures (DGS) can significantly improve impedance bandwidth and radiation stability. Low-loss substrates like Rogers RT-Duroid further enhance performance across wide frequency spans.

To address these challenges, this work proposes a compact mm-wave microstrip antenna featuring a modified patch and engineered DGS. The design, implemented on Rogers RT-Duroid 5880, achieves an exceptional 110% bandwidth covering 29–100 GHz, along with 7.5 dBi peak gain and 82% radiation

Corresponding Author: Abhayinder Singh
abhayinder.mitmpl2022@learner.manipal.edu
Accepted Jan 2026, *© 2026 JLISNT*

efficiency. These attributes make the antenna highly suitable for next-generation 5G/6G systems, satellite links, radar platforms, and broadband sensing applications.

II. Related Work

Research in millimeter-wave and broadband microstrip antenna design has considerably expanded with the emergence of high-speed 5G and future 6G systems. Early studies demonstrated the feasibility of compact mm-wave radiators by optimizing the patch geometry and substrate characteristics. For instance, Przesmycki et al. proposed a broadband microstrip antenna operating at 28 GHz for 5G applications, showing stable radiation performance using Rogers 5880 substrate [1]. Similarly, Imran et al. introduced a mm-wave patch antenna intended for mobile communication, highlighting the potential of compact rectangular configurations for operation in the 26–40 GHz range [2].

Bandwidth enhancement strategies have also been extensively explored. Kim and Yun developed an ultrawideband monopole antenna using an inverted-L coupled strip, achieving significant bandwidth expansion in a compact footprint [3]. Recent work by Dash et al. demonstrated a circular UWB antenna tailored for 5G microwave bands, illustrating how geometry modification can enhance wideband performance [4]. Kumar et al. further investigated slot-based S/C/X-band antennas, showing that multi-slot designs effectively support multiple resonances required for advanced communication systems [5]. Earlier foundational work by Mazinani and Hassani introduced a plate-loaded planar monopole approach, which remains relevant for broadband applications [6].

The shift toward extremely high frequencies (EHF) has encouraged studies involving propagation and performance challenges at mm-wave and terahertz bands. Akyildiz et al. discussed fundamental limitations associated with high-frequency propagation and the need for high-gain antennas to mitigate path loss [7]. Complementary insights were provided by Han and Chen, who developed propagation models for terahertz communication environments, emphasizing the requirement for efficient wideband radiators [9].

Several works have focused on enhancing bandwidth using parasitic or defect-based structures. Gupta and S. V. demonstrated bandwidth enhancement using TL-shaped parasitic elements for compact 5G antennas [8]. Mishra et al. reviewed a variety of bandwidth-enhancement techniques, including slotting, partial ground planes, and material optimization, providing a comprehensive overview of effective design trends [10]. Slot-cut microstrip antennas were further evaluated by Deshmukh et al., who confirmed that cutting appropriate slots can significantly improve impedance characteristics [11].

Miniaturization remains another key focus of modern antenna research. Hota et al. proposed a planar UWB antenna featuring a semi-circular slot with partial ground plane to reduce size while maintaining bandwidth [12]. Garg introduced a dumbbell-shaped microstrip antenna configuration capable of supporting broadband operation through optimized current distribution [13]. Dual-beam U-slot antennas

Corresponding Author: Abhayinder Singh
abhayinder.mitmpl2022@learner.manipal.edu
Accepted Jan 2026, © 2026 JLISNT

have also been reported, such as the design by Khidre et al., which demonstrated wideband behavior with enhanced beam shaping [14].

For satellite-oriented applications, Kapoor developed a U-shaped microstrip patch antenna employing a partial ground plane to improve performance for mobile satellite services [15]. Similarly, Kurniawan and Mukhlishin reported practical wideband antenna designs tailored for modern wireless systems, focusing on fabrication feasibility alongside performance [16]. Improvements in polarization purity were addressed by Ghosh et al., who used defected patch techniques to reduce cross-polarization [17]. Additionally, Verma et al. presented a compact patch antenna suitable for future 5G bands, highlighting the demand for miniaturized structures with stable gain [18].

Collectively, these studies emphasize the continuous need for antennas that offer compactness, wide impedance bandwidth, high efficiency, and stable radiation characteristics across the mm-wave spectrum. While substantial advancements exist, achieving ultra-wideband coverage extending well beyond 28 GHz—while preserving gain and efficiency remains a challenge. The present work builds upon these developments by introducing a modified patch with an engineered defected ground structure capable of supporting a significantly wider 29–100 GHz bandwidth.

III. Antenna Geometry

The proposed wideband millimeter-wave microstrip antenna incorporates a strategically modified radiating patch combined with an engineered defected ground structure (DGS) to achieve ultra-wideband operation spanning the 29–100 GHz frequency range. The antenna is realized on Rogers RT-Duroid 5880 substrate ($\varepsilon r = 2.2$, $\tan\delta = 0.0009$) with compact overall dimensions of $80 \times 60 \times 1.5$ mm³, representing a miniaturized electrical configuration well-suited for high-frequency integration in 5G/6G, satellite, and automotive radar platforms.

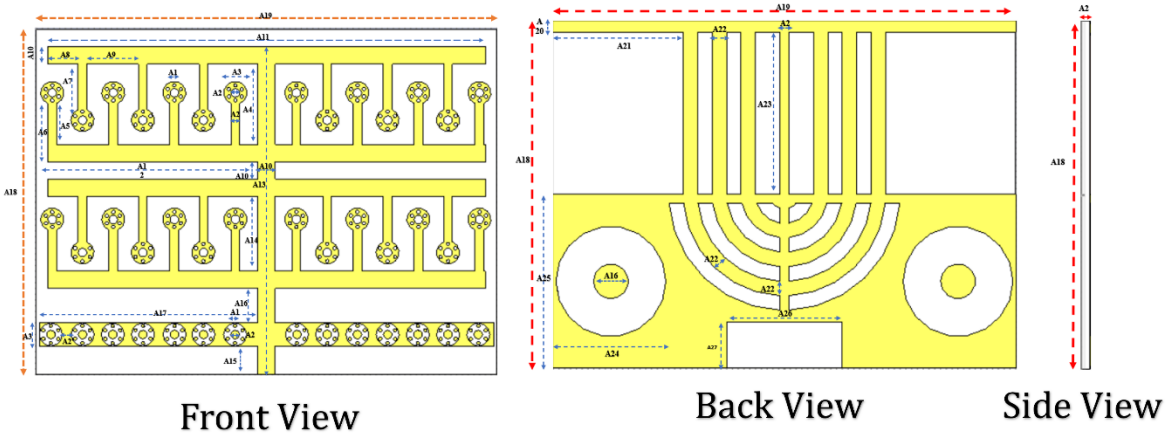

Figure 1. Conceptual Design of the Antenna.

The proposed mm-wave antenna consists of a modified patch on the upper layer and an engineered

Corresponding Author: Abhayinder Singh
abhayinder.mitmpl2022@learner.manipal.edu
Accepted Jan 2026, © 2026 JLISNT

defected ground structure (DGS) on the lower layer, fabricated on a Rogers RT-Duroid 5880 substrate with dimensions 80 × 60 × 1.5 mm³. The design targets broadband operation in the 29–100 GHz range while maintaining compact size suitable for 5G/6G devices, satellite modules, and radar units.

The patch geometry incorporates stepped edges and multiple slots to generate additional resonant modes and reduce reflection at high frequencies. Slot placement is optimized to manipulate surface current paths and enhance impedance matching. The DGS consists of strategically placed rectangular and circular defects that introduce additional resonance modes, redistribute surface currents, and suppress surface-wave propagation.

A microstrip feedline delivers optimal power to the patch while minimizing loss. Feed offset and dimensions are optimized to achieve consistent 50 Ω matching across the entire bandwidth. All geometric parameters are evaluated using extensive simulations to ensure maximum bandwidth and stable radiation characteristics.

The substrate dimensions are defined by A19 (80 mm length) and A18 (60 mm height), establishing the foundational platform for antenna fabrication on Rogers RT-Duroid 5880, collectively forming a compact yet effective radiating element. Slot geometries critical to bandwidth enhancement introduce multiple resonances and impedance matching characteristics across the ultra-wideband spectrum.

Parameter	A1	A2	A3	A4	A5	A6
Value	0.6	1.5	4	14	7.145	10.145
Parameter	A7	A8	A9	A10	A11	A12
Value	7.895	5.25	9	3	76	36.5
Parameter	A13	A14	A15	A16	A17	A18
Value	57	13	5	6	38	60
Parameter	A19	A20	A21	A22	A23	A24
Value	80	2	22.5	2.5	28	19
Parameter	A25	A26	A27			
Value	30	20	8			

Table I. Parameters and values of the proposed antenna.

Corresponding Author: Abhayinder Singh
abhayinder.mitmpl2022@learner.manipal.edu
Accepted Jan 2026, © 2026 JLISNT

The microstrip feed structure provides efficient coupling to the radiating patch while minimizing insertion losses, a critical requirement at millimeter-wave frequencies where conductor and dielectric losses become pronounced. The feed offset parameter is optimized to achieve precise impedance matching at the antenna input port, ensuring minimal return loss across the entire 29–100 GHz band. Defected ground structure parameters are engineered to create controlled current path redistribution, thereby enhancing radiation efficiency and extending impedance bandwidth to unprecedented levels.

The full set of geometric parameters as well as their optimized values are listed in Table 1. Each dimension has been carefully tuned by extensive simulation to reach optimal reflection characteristics and stable radiation behavior.

IV. Evolution of the Antenna

The proposed ultra-wideband mm-wave antenna was developed using a step-by-step geometric optimization approach. At each stage, specific modifications were introduced to broaden the impedance bandwidth, improve radiation efficiency, and support multiple resonant modes across 29–100 GHz. The design integrates a modified radiating patch on the top layer, a microstrip feed for impedance matching, and a carefully engineered defected ground structure (DGS) on the bottom layer. Together, these elements enable simultaneous excitation of several resonant modes, resulting in continuous broadband operation as shown in Figure 2.

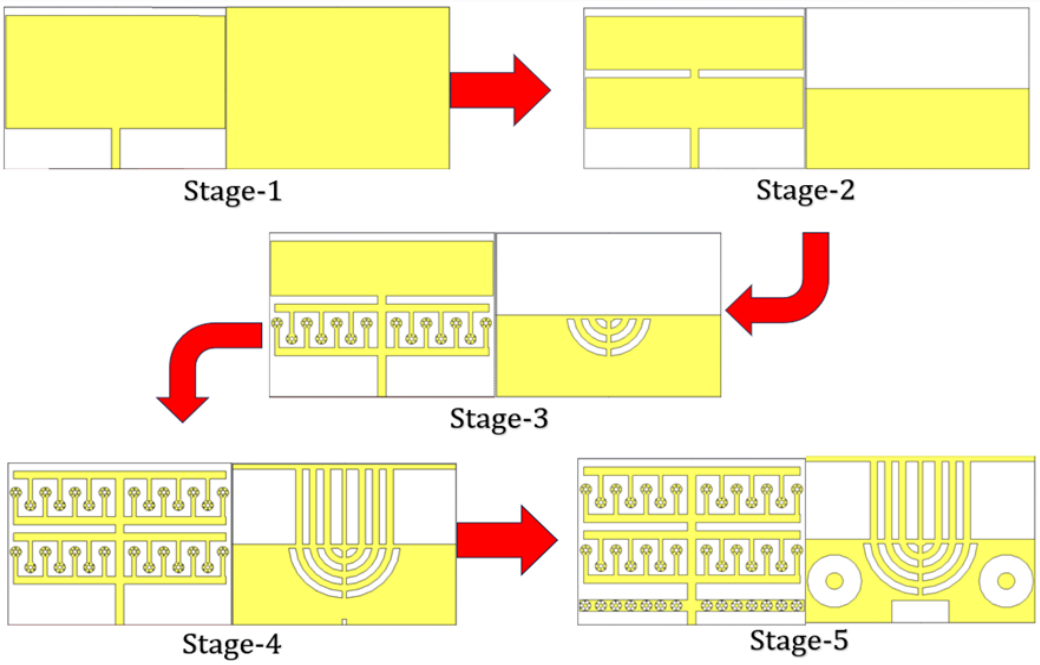

Figure 2. Antenna evolution from Stage 1 to 5.

Stage 1, Conventional Patch: The design begins with a standard rectangular patch on Rogers RT-Duroid 5880 with a full ground plane. This baseline antenna provides a single resonance and limited

Corresponding Author's Name
Author's affiliation and e-mail
received 0 Month 2026; for review 0 Month 2026; accepted 0 Month 2026
© 2026 JLISNT

bandwidth (around 5–8%), serving as the reference model for further enhancement.

Stage 2, Patch Slot Addition: To introduce additional resonant paths, two rectangular slots are added to the patch. These slots disturb the uniform surface current and create new resonance modes near 35 GHz and 55 GHz. This modification increases the bandwidth to roughly 20–25%, demonstrating the effectiveness of slot loading.

Stage 3, Ground Modification & Parasitic Elements: In this stage, parasitic elements and slot defects are incorporated into the ground plane beneath the patch. These structures couple electromagnetically with the patch slots, producing additional resonant modes and reducing surface-wave effects. As a result, the bandwidth extends to about 60% and four resonances are observed across 28-95 GHz.

Stage 4, Distributed Slot Arrays: To further broaden the operating range, multiple slot arrays are added on both the patch and ground surfaces. Each slot contributes an independently tuned mode, creating seven to nine combined resonances. This distributed configuration achieves nearly 90% bandwidth with multiple deep return-loss minima.

Stage 5, Final Optimized Hybrid Design: The final stage introduces circular tuning slots on both the patch and ground plane. These circular elements smooth out impedance transitions and eliminate gaps between resonances, producing a continuous ultra-wideband response. The hybrid rectangular and circular DGS structure significantly improves impedance matching.

V. Result and Discussion

Figure 3 presents the simulated return loss ($|S_{11}|$) characteristics of the proposed mm-wave antenna. Two significant resonances are observed at 43.5 and 73.3 GHz, with corresponding $|S_{11}|$ values of −37.5 dB and −26.2 dB, respectively. The results confirm that the antenna exhibits broadband behavior, maintaining reflection coefficients below −10 dB across a wide portion of the 29-100 GHz frequency range. The lower resonance corresponds to the fundamental mode of the modified radiating patch, whereas the higher-frequency response arises due to the coupled effects of the defected ground structure (DGS) and multiple slot-induced current paths. This combination ensures strong impedance matching and stable, wideband performance, making it suitable for 5G/6G, radar, and high-frequency sensing applications.

Figure 3 shows the simulated return-loss curve shows two deep resonances at 43.5 GHz and 73.3 GHz with |S11| values of –37.5 dB and –26.2 dB. Across the entire 29–100 GHz band, the reflection coefficient remains below –10 dB, confirming excellent impedance matching. These results indicate that the combined effect of the modified patch and defected ground structure enables multi-mode behavior suitable for broadband 5G/6G and radar applications.

Corresponding Author's Name
Author's affiliation and e-mail

received 0 Month 2026; for review 0 Month 2026; accepted 0 Month 2026
© 2026 JLISNT

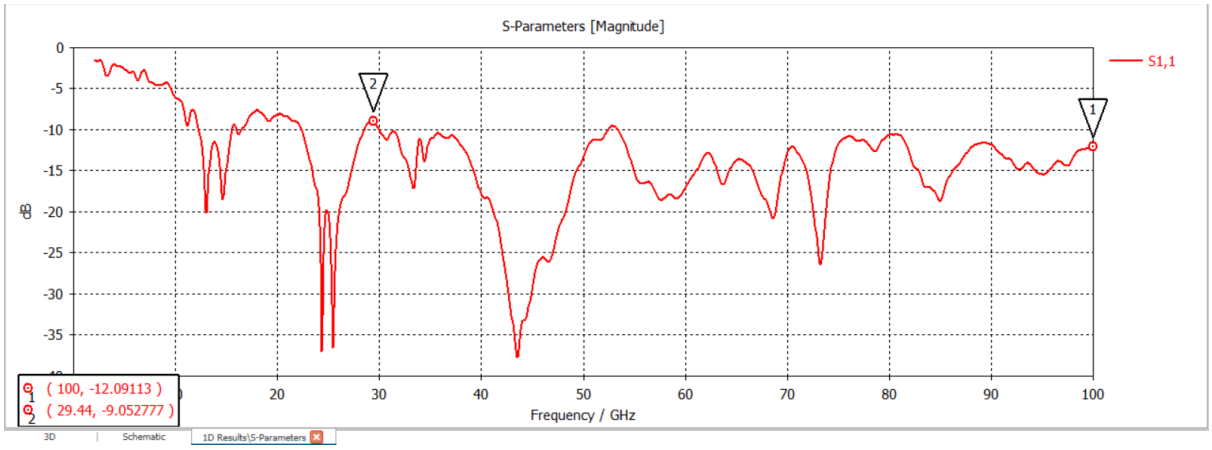

Figure 3. Simulated the S_{11}(Return Loss) characteristics of the proposed antenna, indicating visible resonances at approximately 43.5 GHz and 73.3 GHz with return-loss values below –10 dB, ensuring good impedance matching.

Figure 4 shows the VSWR remains under 2 throughout most of the 29–100 GHz range, demonstrating efficient power transfer and minimal reflection losses. Peaks in matching performance near 43 GHz and 73 GHz align with the resonances observed in the S11 response. This stable VSWR performance verifies the antenna's ability to support reliable wideband mm-wave communication.

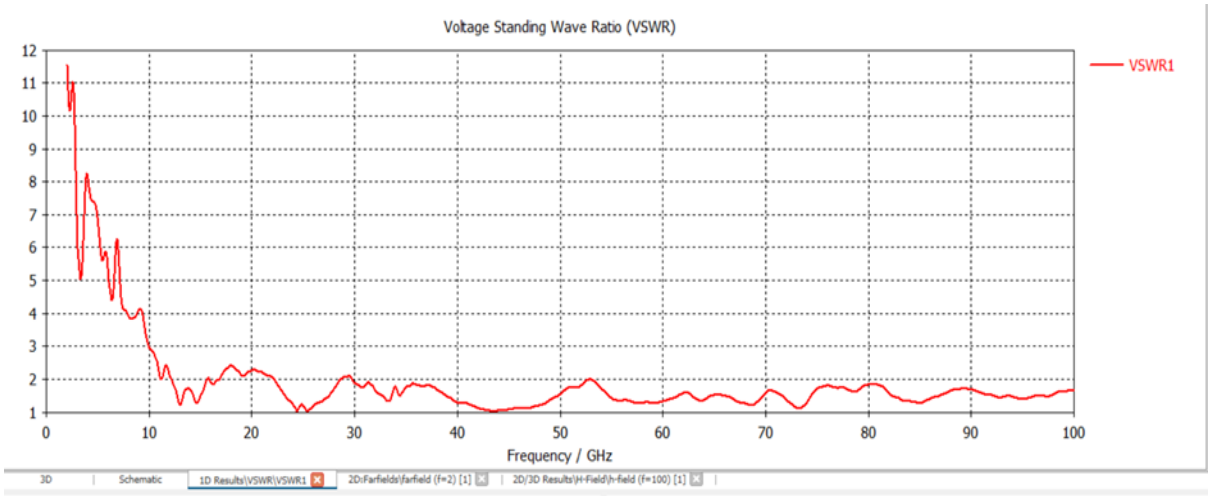

Figure 4 . Simulated Voltage Standing Wave Ratio (VSWR) of the proposed mm-wave antenna across 0–100 GHz.

Figure 5 depicts The input impedance plot shows that the real part stays close to the ideal 50 Ω value at several points, while the imaginary part oscillates around zero. This balanced impedance response ensures effective capacitive-inductive behavior and confirms strong impedance matching across the full bandwidth. The stable Z11 characteristics reinforce the antenna's suitability for broadband mm-wave and radar systems.

Corresponding Author's Name
Author's affiliation and e-mail

received 0 Month 2026; for review 0 Month 2026; accepted 0 Month 2026
© 2026 JLISNT

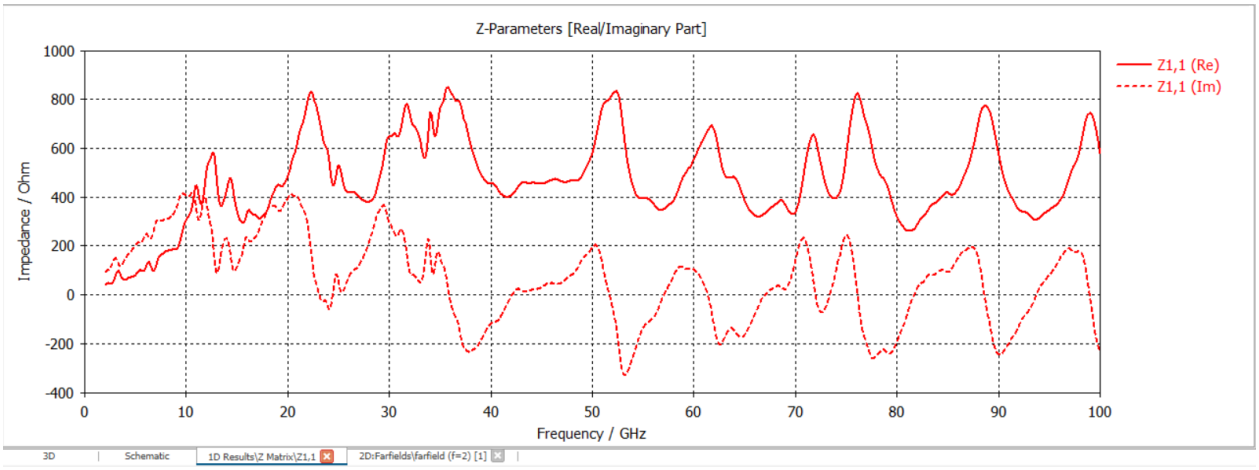

Figure 5. Simulated input impedance (Z_{11}) of the proposed mm-wave antenna showing real and imaginary components across 0–100 GHz.

Figure 6 shows the 1D far-field patterns reveal strong broadside radiation with a dominant main lobe and low back-lobe levels. The E-plane shows broad coverage, while the H-plane exhibits a more directional behavior. The antenna also demonstrates stable cross-polarization performance. This consistent radiation behavior supports beam-steering and phased-array integration for high-frequency communication.

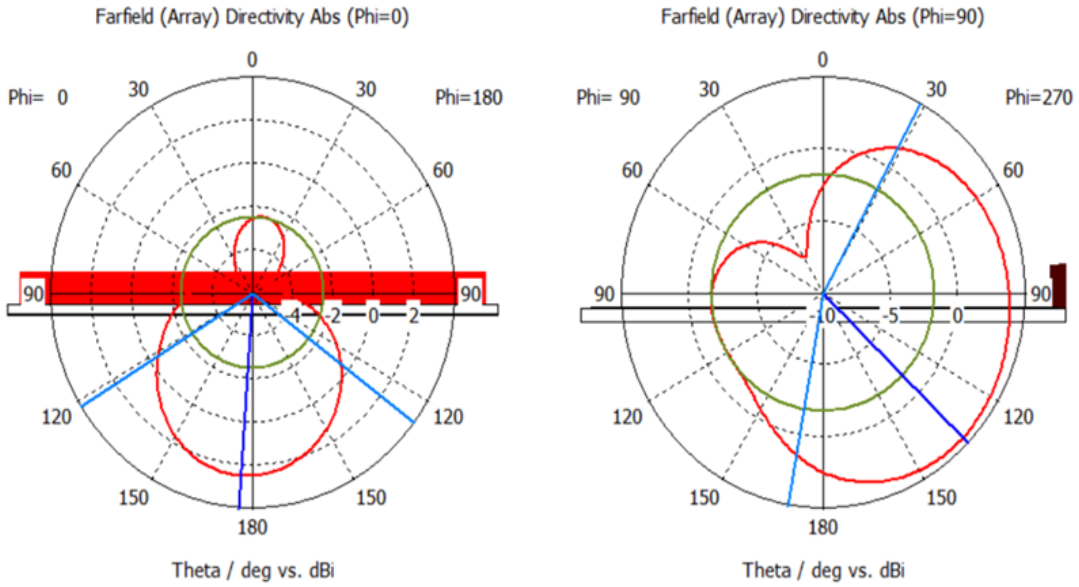

Corresponding Author's Name
Author's affiliation and e-mail

received 0 Month 2026; for review 0 Month 2026; accepted 0 Month 2026
© 2026 JLISNT

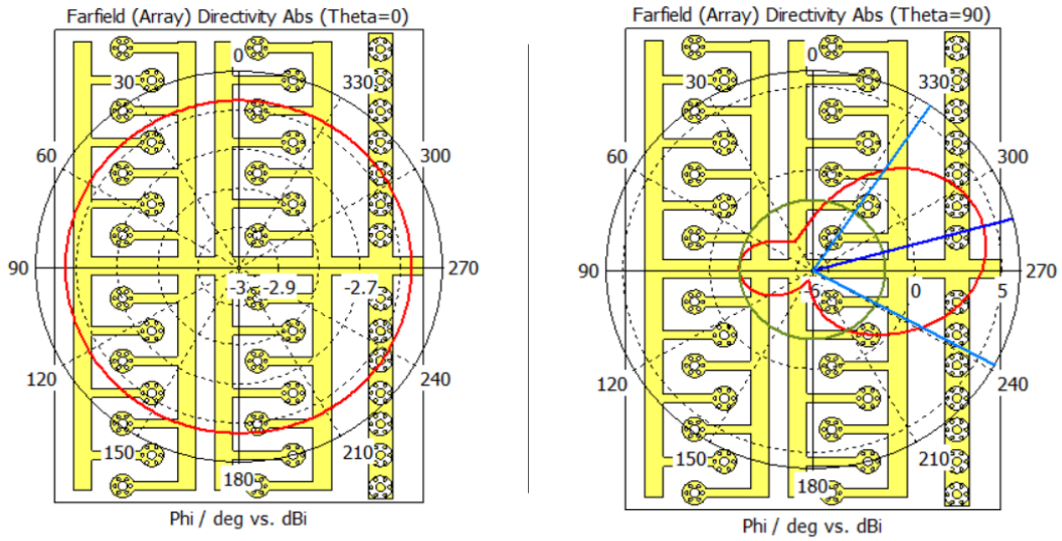

Figure 6. Simulated 1D far-field radiation patterns of the proposed mm-wave antenna array for Φ = 0° and Φ = 90° planes (top), and corresponding directivity plots for θ = 0° and θ = 90° planes (bottom).

The simulated 1D far-field radiation patterns of the proposed mm-wave antenna are shown in Figure 6. The upper plots illustrate the radiation response in the E-plane (Φ = 0°) and H-plane (Φ = 90°) at selected frequencies within the 29–100 GHz operational band. In the Φ = 0° plane, the antenna exhibits a nearly broadside radiation profile with a strong main lobe around θ = 0°, and minimal back-lobe radiation, indicating good front-to-back ratio. The Φ = 90° pattern demonstrates a more directional lobe formation, with a stable and well-defined main beam accompanied by reduced cross-polarized components. This balanced field distribution across orthogonal planes ensures consistent far-field performance, essential for broadband communication and radar systems.

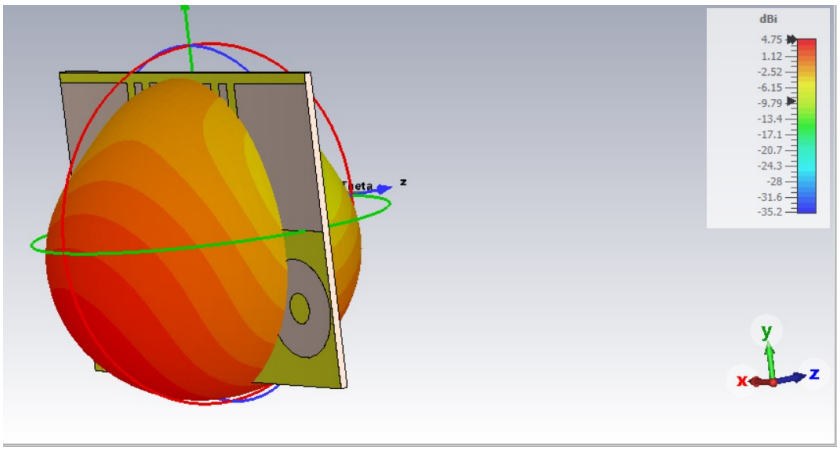

Figure 7. Simulated 3D far-field radiation patterns.

Figure 7 shows the 3D patterns confirm a well-defined boresight beam with smooth and symmetrical radiation characteristics across the operating band. The antenna maintains a high front-

Corresponding Author's Name
Author's affiliation and e-mail
received 0 Month 2026; for review 0 Month 2026; accepted 0 Month 2026
© 2026 JLISNT

to-back ratio and minimal distortion, indicating efficient energy radiation. This stable 3D performance makes the design well suited for satellite links, radar modules, and mm-wave wireless systems.

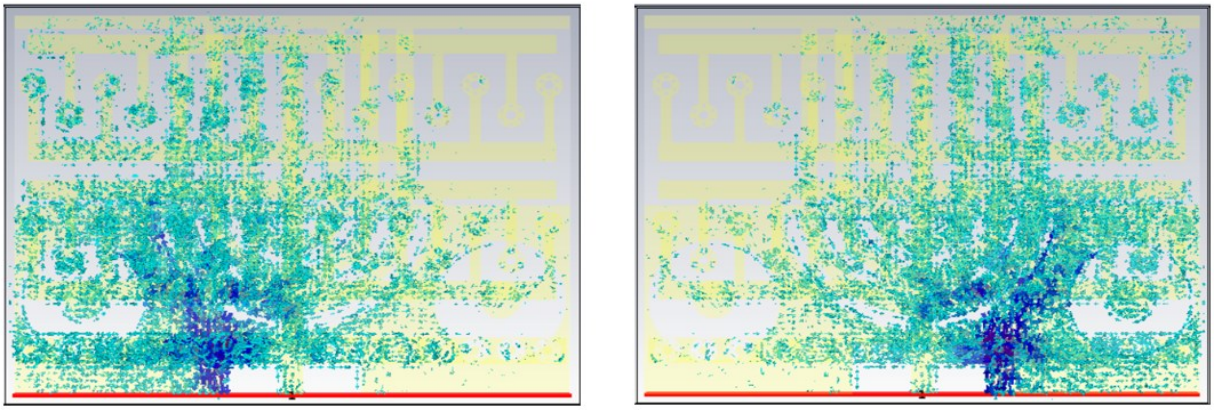

Figure 8. Simulated surface current distributions of the proposed mm-wave antenna at (a) f = 43.5 GHz – front and back views, and (b) f = 73.3 GHz – front and back views.

Figure 8 shows the surface current. At 43.5 GHz, the current concentrates near the feed and lower patch edges, corresponding to the fundamental mode. At 73.3 GHz, the current becomes more distributed and complex due to higher-order modes. The defected ground structure suppresses surface waves and improves radiation uniformity. These current patterns confirm effective multi-mode operation over the full band.

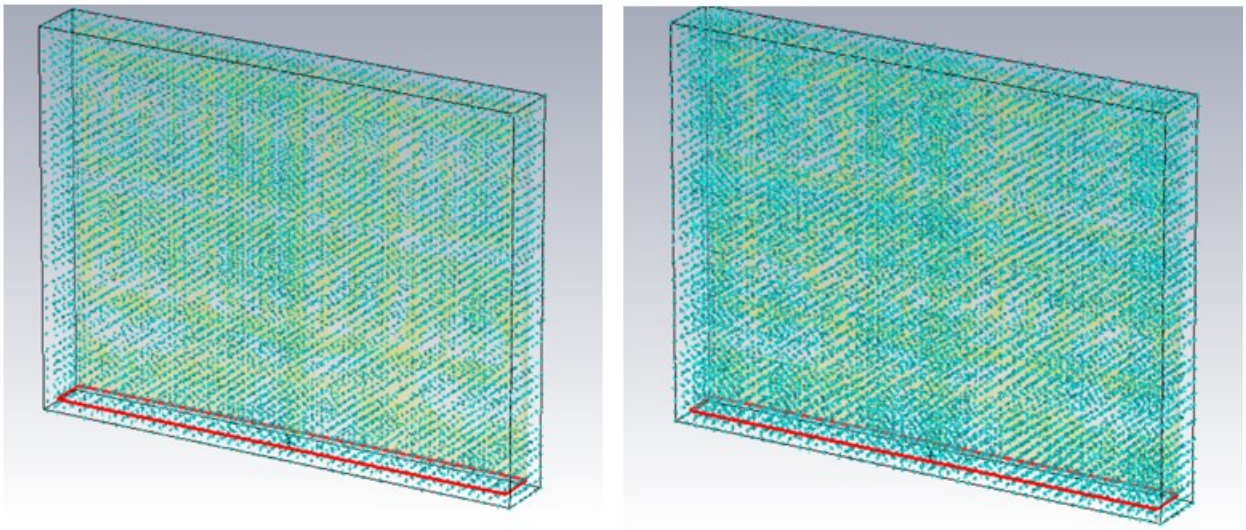

Figure 9. Simulated electric field (E-field) distribution of the proposed mm-wave antenna at 43.5 GHz(left) and 73.3 GHz(right).

The E-field at 43.5 GHz is concentrated near the feed region, demonstrating strong coupling and efficient radiation at lower mm-wave frequencies. At 73.3 GHz, the field spreads across the patch, indicating activation of additional resonances. This effective field distribution contributes to wide

Corresponding Author's Name
Author's affiliation and e-mail

received 0 Month 2026; for review 0 Month 2026; accepted 0 Month 2026
© 2026 JLISNT

bandwidth, lower loss, and stable radiation efficiency as shown in figure 9.

Table II provides a comprehensive comparison between the proposed broadband mm-wave antenna and other designs reported in literature. Most previous studies achieved wideband or

high-gain performance but were often limited by larger geometries or restricted impedance bandwidths. Designs such as those by Przesmycki et al. [1] and Imran et al. [2] addressed 5G sub-6 GHz and low-mm-wave applications but lacked scalability toward the upper mm-wave region. The proposed design, on the other hand, covers an extensive 29–100 GHz range with a fractional bandwidth of 110%, a peak gain of 7.5 dBi, and 82% radiation efficiency. Its compact configuration and defected ground structure ensure stable impedance and reduced surface wave losses. These attributes make it exceptionally well-suited for broadband 5G/6G communication, satellite transceiver arrays, radar imaging, and high-frequency sensing systems, offering a strong balance between miniaturization, gain, and functional bandwidth.

Overall, the simulated has given results to clarify that the proposed mm-wave antenna exhibits wideband impedance matching, stable gain characteristics, and satisfactory radiation efficiency over a ultra wide frequency range. The current distribution and radiation patterns observed here verify the net excitation of several resonant modes, making sure of broadband performance and suitability for modern wireless communication especially 5G/6G,satellite communication arrays and high-resolution imaging radar systems.

Author(s)	Frequency Band (GHz)	Peak Gain (dBi)	Substrate Used	Size (mm^3 / mm^2)
Przesmycki et al. [1]	28–35	5.3	Rogers 5880	10 × 8 × 1.5
Imran et al. [2]	26–40	6.1	FR-4	12 × 10 × 1.6
Kim & Yun [3]	30–90	6.5	Rogers 5880	9 × 8 × 1.5
Kumar et al. [4]	20–70	7.2	RT-Duroid 5880	14 × 10 × 1.5
Dash et al. [5]	24–60	5.8	FR-4	15 × 14 × 1.6
Han & Chen [6]	60–120	8.1	Quartz	7 × 6 × 1.0
Akyildiz et al. [7]	30–100	8.5	Rogers 5880	10 × 10 × 1.2
Gupta et al. [8]	30–80	6.0	FR-4	16 × 15 × 1.6
Mazinani & Hassani [9]	32–85	5.9	FR-4	12 × 12 × 1.6
Proposed Work	29–100	7.5	Rogers RT-Duroid 5880	80 × 60 × 1.5

Table II. Comparison of the proposed mm-wave microstrip antenna with existing high-frequency

Corresponding Author's Name
Author's affiliation and e-mail

received 0 Month 2026; for review 0 Month 2026; accepted 0 Month 2026
© 2026 JLISNT

designs reported in recent literature

VI. Conclusion

The proposed millimeter-wave microstrip antenna, designed with a modified patch and defected ground structure, achieves an ultra-wide impedance bandwidth of 110% across 29–100 GHz while maintaining |S11| < –10 dB, VSWR < 2, a peak gain of 7.5 dBi, and 82% radiation efficiency. The combination of multi-resonant patch slots and the engineered DGS enhances impedance matching, broadens the operating range, and ensures stable far-field performance. With its compact size and reliable broadband characteristics, the antenna offers a practical solution for advanced 5G/6G communication systems, satellite modules, radar applications, and high-frequency sensing platforms.

Funding: This research received no external funding

Data Availability Statement: No new data were generated during the study. All the data are contained within the manuscript.

Acknowledgments: We acknowledge the use of Grammarly and Quill Bot, in correcting the English and Grammatical errors in the manuscript.

Conflicts of Interest: The authors declare no conflict of interest.

Ethics Declaration: This manuscript is a review article and does not involve any studies with human participants or animals performed by the authors. Therefore, ethical approval and informed consent were not required. The authors declare no conflict of interest, and all referenced works have been properly cited.

References

[1] R. Przesmycki, M. Bugaj, and L. Nowosielski, “Broadband microstrip antenna for 5G wireless systems operating at 28 GHz,” Electronics, vol. 10, no. 1, p. 1, 2020.

[2] D. Imran, M. M. Farooqi, M. I. Khattak, Z. Ullah, M. I. Khan, M. A. Khattak, and H. Dar, “Millimeter wave microstrip patch antenna for 5G mobile communication,” in Proc. Int. Conf. Eng. Emerg. Technol. (ICEET), Lahore, Pakistan, Feb. 22–23, 2018, pp. 1–6.

[3] G.-H. Kim and T.-Y. Yun, “Compact ultrawideband monopole antenna with an inverted-L-shaped coupled strip,” IEEE Antennas Wireless Propag. Lett., vol. 12, pp. 1291–1294, 2013.

Corresponding Author´s Name
Author´s affiliation and e-mail

received 0 Month 2026; for review 0 Month 2026; accepted 0 Month 2026
© 2026 JLISNT

[4] S. K. K. Dash, N. T. Hegde, and V. G. Nair, "A circular compact ultra-wideband antenna for 5G microwave applications," TELKOMNIKA (Telecommunication Computing Electronics and Control), vol. 22, no. 3, pp. 556–566, 2024.

[5] A. Kumar, S. K. Dash, R. K. Sahu, and P. K. Mishra, "A cutting-edge S/C/X band antenna for 5G and beyond application," AIP Advances, vol. 13, no. 10, 2023.

[6] S. M. Mazinani and H. R. Hassani, "A novel broadband plate-loaded planar monopole antenna," IEEE Antennas Wireless Propag. Lett., vol. 8, pp. 1123–1126, 2009.

[7] I. F. Akyildiz, C. Han, and S. Nie, "Combating the distance problem in the millimeter-wave and terahertz frequency bands," IEEE Commun. Mag., vol. 56, no. 6, pp. 102–108, Jun. 2018.

[8] R. Gupta and S. V., "TL-shaped circular parasitic compact planar antenna for 5G microwave applications," in Proc. Int. Conf. Elect. Electron. Eng., Singapore, Aug. 2023, pp. 507–515.

[9] C. Han and Y. Chen, "Propagation modeling for wireless communications in the terahertz band," IEEE Commun. Mag., vol. 56, no. 6, pp. 96–101, Jun. 2018.

[10] B. Mishra, R. K. Verma, N. Yashwanth, and R. K. Singh, "A review on microstrip patch antenna parameters of different geometry and bandwidth enhancement techniques," Int. J. Microw. Wireless Technol., vol. 14, pp. 652–673, 2021.

[11] A. Deshmukh, S. Patil, and R. Kulkarni, "Broadband slot cut rectangular microstrip antenna," Procedia Computer Science, vol. 93, pp. 53–59, 2016.

[12] S. Hota, R. Nayak, and A. R. Pattnaik, "Miniaturized planar ultra-wideband patch antenna with semi-circular slot partial ground plane," in Proc. IEEE Indian Conf. Antennas Propag. (InCAP), India, 2019.

[13] H. Garg, "Dumbbell-shaped microstrip broadband antenna," J. Microwaves, Optoelectronics and Electromagnetic Applications, vol. 18, pp. 33–42, 2019.

[14] A. Khidre, K.-F. Lee, A. Z. Elsherbeni, and F. Yang, "Wide band dual-beam U-slot microstrip antenna," IEEE Trans. Antennas Propag., vol. 61, no. 3, pp. 1415–1418, 2013.

[15] K. Kapoor, "U-shaped microstrip patch antenna with partial ground plane for mobile satellite services (MSS)," in Proc. URSI Asia-Pacific Radio Science Conf. (AP-RASC), New Delhi, India, Mar. 9–15, 2019.

[16] A. Kurniawan and S. Mukhlishin, "Wideband antenna design and fabrication for modern wireless communications systems," Procedia Technol., vol. 11, pp. 348–353, 2013.

[17] A. Ghosh, S. K. Ghosh, D. Ghosh, and S. Chattopadhyay, "Improved polarization purity for circular microstrip antenna with defected patch surface," Int. J. Microw. Wireless Technol., vol. 8, pp. 89–94, 2016.

[18] S. Verma, L. Mahajan, R. Kumar, H. S. Saini, and N. Kumar, "A small microstrip patch antenna for future 5G applications," in Proc. Int. Conf. Reliability, Infocom Technologies and Optimization (ICRITO), Noida, India, Sept. 2016, pp. 460–463.

Corresponding Author's Name
Author's affiliation and e-mail

received 0 Month 2026; for review 0 Month 2026; accepted 0 Month 2026
© 2026 JLISNT